

Polypeptide grafted macroporous PolyHIPE by Surface Initiated N-carboxyanhydride Polymerization as a platform for bioconjugation.

Fabrice Audouin¹, Mary Fox², Ruth Larragy², Jin Huang¹, Brendan O'Connor², Andreas Heise^{1*}

¹School of Chemical Sciences, Dublin City University, Glasnevin, Dublin 9, Ireland.

²Irish Separation Science Cluster, Dublin City University, Glasnevin, Dublin 9, Ireland

KEYWORDS (Word Style "BG_Keywords"). If you are submitting your paper to a journal that requires keywords, provide significant keywords to aid the reader in literature retrieval.

Supporting Information Placeholder

ABSTRACT: A new class of functional macroporous monoliths from polymerized high internal phase emulsion (polyHIPE) with tunable surface functional groups was developed by direct polypeptide surface grafting. In the first step, amino-functional polyHIPEs were obtained by the addition of 4-vinylbenzyl or 4-vinylbenzylphthalimide to the styrenic emulsion and thermal radical polymerization. The obtained monoliths present the expected open-cell morphology and a high surface area. The incorporated amino group was successfully utilized to initiate the ring opening polymerization of benzyl-L-glutamate N-carboxyanhydride (BLG NCA) and benzyloxycarbonyl-L-lysine (Lys(Z)) NCA, which resulted in a dense homogeneous coating of polypeptides throughout the internal polyHIPE surfaces as confirmed by SEM and FTIR analysis. The amount of polypeptide grafted to the polyHIPE surfaces could be modulated by varying the initial ratio of amino acid NCA to amino-functional polyHIPE. Subsequent removal of the polypeptide protecting groups yielded highly functional polyHIPE-g-poly(glutamic acid) and polyHIPE-g-poly(lysine). Both type of polypeptide-grafted monoliths responded to pH by changes in their hydrophilicity. The possibility to use the high density of function (-COOH or -NH₂) for secondary reaction was demonstrated by the successful bioconjugation of enhanced green fluorescent protein (eGFP) and fluorescein isocyanate (FITC) on the polymer 3D-scaffold surface. The amount of eGFP and FITC conjugated to the polypeptide grafted polyHIPE was significantly higher than to the amino-functional polyHIPE signifying the advantage of polypeptide grafting to achieve highly functional polyHIPEs.

INTRODUCTION

Macroporous polymeric monoliths combining high surface area with excellent flow and mass transport properties are ideally suited for a variety of applications including column filtration/separation, supported organic chemistry and as media for tissue engineering and 3D cell culture.^{i-viii} A material that has received increased attention as a microcellular polymer monolith is prepared from concentrated high internal phase emulsions (HIPE) containing more than 74% internal phase volume. If the continuous phase contains one or more monomeric species and polymerization is initiated, highly porous materials referred to as polyHIPEs are produced once the dispersed phase droplets are removed. Initially developed by Unilever^{ix}, polyHIPE preparation traditionally involves the formation of a stable concentrated water-in-oil emulsion using hydrophobic monomers as part of the continuous phase and an aqueous phase as the dispersed phase.^{x,xi} The preparation of the so-called "reverse" polyHIPE by polymerization of an oil-in-water HIPE was also developed during the last decade.^{xii-xix}

Essential to opening new polyHIPE applications areas in biosensing and bioseparation is the ability to conveniently functionalize and (bio)conjugate polyHIPE surfaces. The functionalization of polyHIPEs has been achieved by adding a functional comonomer to the emulsion.^{xx-xxii} However, this monomer should be sufficiently hydrophobic not to destabilize the emulsion and this considerably limits the choice of potentials

candidates. A second method is based on the post-functionalization of unreacted double bonds on the polyHIPE surface, but only low degrees of surface functionalization have been realized.^{xxiii,xxiv} A more promising approach to conveniently modify polyHIPEs with a high density of functional groups is the grafting of functional polymers from the polyHIPE surface. Polymer brushes covalently attached to surfaces possess excellent mechanical and chemical robustness and offer the flexibility to introduce a large variety of functional monomers at high functionalization density.^{xxv} Currently only few publications discuss the modification of the polyHIPE surface with polymer brushes. In initial reports we as well as Maillard disclosed the incorporation of a polymerizable initiator for atom transfer radical polymerization (ATRP) into a pHIPE and the subsequent surface grafting reaction by *in situ* ATRP of methyl methacrylate (MMA).^{xxvi,xxvii} We later extended this approach to the grafting of glycidyl methacrylate (GMA) resulting in highly functional polyHIPE, which could be used as a reactive platform for example for "click" chemistry to efficiently decorate the polyHIPE surface.^{xxviii} Alternatively we are now interested in the grafting of synthetic polypeptides due to their biocompatibility and functionality through the choice of amino acids.^{xxix} Moreover, synthetic polypeptides have shown to be pH responsive, which opens possibilities to introduce responsiveness into polyHIPE monoliths.^{xxx} Polypeptides are also useful platforms for various modification chemistries allowing secondary modifications

and functionalizations.^{xxx-xxxv} We thus anticipated that grafting polypeptides onto the polyHIPE surface would give rise to novel and advanced materials.

Well-defined synthetic polypeptides based on natural and non-natural amino-acids have successfully been synthesized by the ring opening polymerization of their N-carboxyanhydrides (NCAs).^{xxxvi-xli} While different techniques to control the NCA polymerization have been reported^{xlii-xliii}, primary amines are the most widely used initiators for this polymerization.^{xliv} We hypothesized that growth of polypeptide chains from a polyHIPE surface could be achieved by attaching the initiating sites, i.e. primary amines onto a surface followed by *in situ* ROP of the NCA monomers. Here we disclose a new class of primary amine functional macroporous polyHIPEs (polyHIPE-NH₂) by the incorporation of a polymerizable monomer with a pendant amino group into a styrene/divinylbenzene HIPE formulation. The grafted initiator was successfully used for the polymerization of γ -benzyl-L-glutamate (BLG) NCA and benzyloxycarbonyl-L-lysine (Lys(Z)) NCA resulting in a dense coating of polypeptides on the polyHIPE surface. After in-situ deprotection both polypeptide functionalized polyHIPEs were rendered pH responsive. Moreover, the availability of the high density of functional groups on the polyHIPE surface for bioconjugation was studied by the covalent attachment of a green fluorescent protein to the poly(glutamic acid) coated polyHIPE.

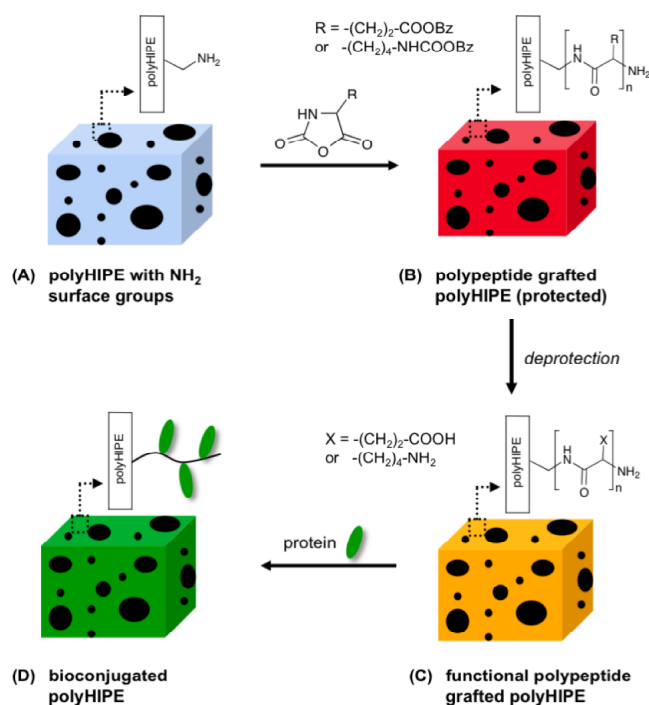


Figure 1. Synthetic pathway to polypeptide grafted polyHIPE and subsequent bioconjugation.

EXPERIMENTAL METHODS

Materials. Hypermer B246 was a gift from CRODA UK. Dipotassium peroxodisulfate 97% was purchased from BDH Limited Poole England. All others chemicals were purchased from Sigma-Aldrich and used as received unless otherwise noted. Iodotrimethylsilane (TMSI), dimethylchloromethane and anhydrous chloroform were used directly from the bottle under an inert and dry atmosphere. Benzyloxycarbonyl-L-

lysine and γ -benzyl-L-glutamate were purchased from Bachem. ϵ -Benzyloxycarbonyl-L-lysine NCA and γ -benzyl-L-glutamate NCA were synthesized following a literature procedure.^{xlv} 4-vinylbenzylphthalimide and 4-vinylbenzylamine were synthesized following a literature procedure.^{xlvi} **GFP**

Methods. Specific surface area N₂ adsorption measurements were performed on a Micromeritics ASAP 2010 V4 analyzer (Normass, GA) and the data were subjected to the Brunauer-Emmett-Teller (BET) treatment.^{xlvii} The final porosity and pore size distribution were determined with an Autopore IV 9500 porosimeter from Micromeritics. Scanning electron microscopy (SEM) and energy dispersive X-ray (EDX) were performed on a Hitachi S3400 with samples previously coated with gold using vapour deposition in the case of SEM analysis. Fourier Transform InfraRed (FTIR) spectroscopy was done in solid state on a Perkin Elmer Spectrum 100. Wettability tests of polyHIPEs was performed using a FTÅ200 dynamic contact angle analyser and on dried samples. Elemental analysis was performed on an Exeter Analytical CE440 elemental analyser and a Varian 55B SpectroAA atomic absorption spectrometer. Fluorescence microscopy images of polyHIPE-g-PLys labeled FITC were obtained using an inverted microscope (Olympus IX81) equipped with a CCD camera (Hamamatsu C4742-80-12AG) and a xenon lamp as the light source. Images were collected with a 4x objective (excitation filter BP492/18; emission light was collected through a filter cube, U-MF2, Olympus). An inverted fluorescence microscope (IX81, Olympus Co., Japan) equipped with an EMCCD camera (DV887-BI, Andor Technology, UK) and an MT20 fluorescence illumination unit fitted with a 150 W xenon lamp was used in combination with a FITC filter set to image the green fluorescence of the eGFP immobilized onto the polyHIPE-g-PGA. The fluorescent images were acquired using the Cell^R software (Olympus Soft Imaging Solutions, GmbH, Germany), and all fluorescent images were acquired using the same set of parameters.

Synthesis of polyHIPE-NH₂: For example (sample P1 from table 1), 1.7 g (0.0163 mol) of styrene, 0.7 g (0.0053 mol) of divinylbenzene, 0.4 g (0.0015 mol) of 4-vinylbenzylphthalimide and 0.8 g of Span 80 surfactant were placed in a reactor and the mixture stirred using an overhead stirrer at 300 rpm. The aqueous solution was prepared by dissolving 0.3 g of potassium peroxodisulfate (K₂S₂O₈) in 25.5 ml of deionised water and 17 ml of the prepared aqueous solution was used as the internal phase. It was added dropwise to the monomer solution under constant stirring. Once all aqueous phase was added, stirring was continued for a further 20 minutes to produce a uniform emulsion. Afterwards, the emulsion was transferred to **mould in glasses** and heated at 60°C for 24 hours. The resulting monoliths were washed with THF (3*250ml), then acetone (2*250ml) before drying *in vacuo* at 40°C overnight. **DO WE NEED A PROCEDURE FOR 4-VINYLBENZYLAMINE?**

The phthalimide group was removed by the following procedure. The polyHIPE (500 mg) was vigorously stirred in a solution of 150 ml ethanol containing tertbutylalcohol (60 mg). Then, 5 ml of hydrazine monohydrate was added and the solution was heated under reflux during 24 hours. Afterwards the polyHIPE was washed three times with 150 ml of ethanol before drying *in vacuo*. For the polyHIPEs synthesized from the 4-vinylbenzylamine, a similar washing procedure was applied omitting the step of deprotection. All composition used in the polyHIPEs synthesis are listed in Table 1.

Table 1. Compositions used for the synthesis of amine-functional polyHIPEs (S: styrene; DVB: divinylbenzene; AM: amine monomer).

polyHIPE	Continuous phase				Dispersed phase	
	AM (g)	S (g)	DVB (g)	Surfactant (g)	H ₂ O (ml)	K ₂ S ₂ O ₈ (g)
P1	0.4 ^a	1.7	0.7	0.8 ^c	17	0.2
P2 ^e	0.8 ^a	1.3	0.7	0.8 ^c	14.6	0.2
P3	0.4 ^a	1.7	0.7	0.4 ^d	17	0.2
P4	0.3 ^b	1.7	0.7	0.8 ^c	17	0.2
P5	0.3 ^b	1.7	0.7	0.4 ^d	17	0.2

(a) 4-vinylbenzylphthalimide. (b) 4-vinylbenzylamine (c) Span 80 (d) Hypermer B246 (e) 2.4 mL toluene was added to this formulation as porogen.

Synthesis of polyHIPE-g-PBLG and polyHIPE-g-PLys(Z). PolyHIPE-NH₂ (40 g) was placed in a Schlenk tube with 4 ml of anhydrous chloroform under nitrogen. γ -Benzyl-L-glutamate-NCA (200 mg) was dissolved in 5 ml of anhydrous chloroform under inert atmosphere. This solution was added to the polyHIPE-NH₂ with a cannula under N₂. The reaction was left to stand at room temperature for 48 h. The monolith was washed with (3*250 ml) DMF to remove unreacted monomer and free polymer. Then, it was washed with acetone (2*250 ml) and dried under vacuo for 24 h. The same procedure was used to synthesize the polyHIPE-g-PLys(Z) from ϵ -benzyloxycarbonyl-L-lysine NCA.

Conversion of PHIPE-g-PLys(Z) and PHIPE-g-PBLG into PHIPE-g-PLL and PHIPE-g-PGA. The polyHIPE-g-PLys(Z) was converted into polyHIPE-g-poly(L-lysine) (polyHIPE-g-PLys) using HBr/TFA deprotection. PolyHIPE-g-PLys(Z) (40 gm) was stirred overnight with 6 ml of trifluoroacetic acid (TFA) and 0.1 ml of hydrobromic acid solution (HBr). Then, the material was washed 4 times with 30 ml of DMF and 2 times with 30 ml of acetone and dried under vacuo.

The polyHIPE-g-PBLG was converted into polyHIPE-g-poly(L-glutamic acid) (polyHIPE-g-PGA) using two different methods of deprotection: (1) For HBr/TFA, the protocol was similar to the polyHIPE-g-PLys(Z). (2) For TMSI, 40 mg of polyHIPE-g-PBLG was stirred in 16 ml of anhydrous dichloromethane (DCM) and 100 μ l of iodotrimethylsilane under nitrogen at 40°C during 24 hours. Then, the material was washed with 30 ml of DCM and 30 ml of THF 3 times and dried under vacuo.

Grafting fluorescein isocyanate onto polyHIPE-g-PLL and polyHIPE-NH₂

PolyHIPE-g-PLys (5 mg) was mixed in the dark during 24 hours with 1 ml of DMF and 5 ml of buffered solution (pH = 9.2) containing 20 mg of fluorescein isocyanate (FITC). The final polyHIPE-g-PLys labelled FITC was washed in the dark with 10 ml of buffered solution/DMF (5:1 in v/v) 3 times and 2 times with 10 ml of acetone and dried under vacuo. The same procedure was applied to polyHIPE-NH₂.

Enhanced green fluorescent (eGFP) protein immobilization.

The experimental conditions for the eGFP immobiliza-

tion onto polyHIPE-g-PGA are given in Table 2. For all experiments except PGFP5, polyHIPE-g-PGA was pre-treated with sodium hydroxide: 20 mg of the polyHIPE-g-PGA was vigorously stirred in 10 ml of DI water and a solution of 0.1 M NaOH was added drop-wise until the pH of the solution turned to 11-12. After 15 minutes, the material was washed with DI water until the pH returned to neutral followed by drying of the material. For the eGFP conjugation, 2.5 mg of polyHIPE-g-PGA was mixed with 0.5 mg of N-hydroxysulfosuccinimide sodium salt (sulfo-NHS) in 0.49 ml of phosphate buffered saline (PBS, pH = 7.4). Then, a solution of 1 mg of 1-ethyl-3-(3-dimethylaminopropyl) carbodiimide hydrochloride (EDC) in 0.5 ml PBS was added and mixed together for 30 min. Afterwards, 2 ml of eGFP in PBS (1.5 mg of protein per 1 ml of PBS) and 10 μ l 4-(dimethylamino)pyridine (DMAP) in PBS solution (1 mg of DMAP per 1 ml PBS) were added and the solution stirred for 2 days at room temperature. The material was subsequently washed extensively with the same buffer solution to remove any unbound protein, then with DI water and dried under vacuo at room temperature for 24 hours.

Table 2 Experimental conditions for the eGFP immobilization onto polyHIPE-g-PGA (entry code denotes polyHIPE-g-PGA used, e.g. P1GPF = P1-PGA) WHICH NCA RATIO?

Entry	pHIPE-g-PGA (mg)	eGFP buffer (ml)	Sulfo-NHS (mg)	EDC (mg)	DMAP (mg)	Buffer (ml)
P1GFP	3.5	1 ^{a[1.5]}	0.5	1	0.01	2 ^a
P2GFP	3.5	1 ^{b[1.9]}	0.5	1	-	2 ^b
P3GFP	2.5	2 ^{a[1.5]}	0.5	1	0.01	1 ^a
P4GFP	2.5	2 ^{b[1.9]}	0.5	1	-	1 ^b
P4GFP*	2.5	1 ^{a[1.5]}	0.5	1	0.01	2 ^a

* PGA conjugation without prior NaOH treatment. (a) PBS buffer solution pH = 7.4. (b) Sodium carbonate buffer solution pH = 8.6 [x] eGFP concentration in mg/ml.

RESULTS AND DISCUSSION

PolyHIPE-NH₂ synthesis

The synthesis of polypeptide-grafted polyHIPEs by NCA polymerization requires the chemical incorporation of an amine initiator group into the polyHIPE surface (Figure 1). The critical step in this process is the development of a stable HIPE formulation in the presence of a polymerizable monomer containing a free or protected amine. Based on our previous work on the combination of free radical and NCA polymerization^{xlvi}, we selected 4-vinylbenzylamine as the amine functional monomer. A comparison was made between its direct incorporation into the styrene/DVB-based emulsion with that of its protected equivalent (4-vinylbenzylphthalimide). The obtained results showed that the choice of surfactant is essential for the successful synthesis of stable HIPEs containing a sufficient amount of both functional monomers and the corresponding polyHIPE with a well-defined morphology. The two surfactants used as the emulsion stabilizer were sorbitan monooleate (Span 80, HLB = 4.3), a surfactant commonly employed in the production of W/O HIPEs^{xxiv,xlviii-liv} and a non-ionic surfactant ABA block copolymer (Hypermer B246, HLB = 5-6) reported to generate stable W/O HIPEs with functional acrylic monomers^{xxv,lv} (formulation compositions see Table 1). In all cases the HIPE formed

successfully and no obvious signs of phase separation were observed suggesting that the emulsions were stable up to the point of gelation.

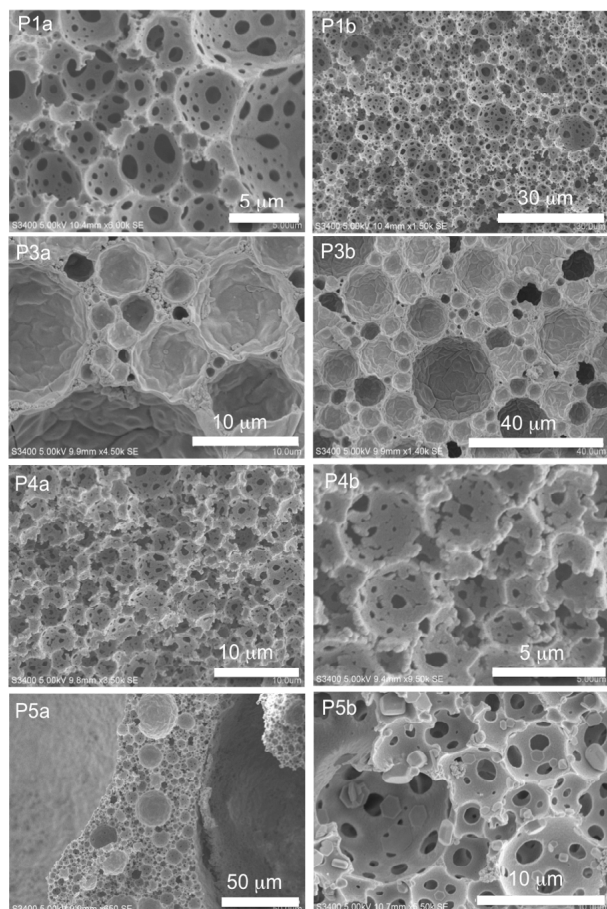


Figure 2. SEM images of amino functionalized polyHIPEs. Labels (e.g. P1) refer to entries in Table 1 and Table 2.

The morphology of the resulting polyHIPE materials, after thermal polymerization at 70°C, was investigated by Scanning Electron Microscopy (SEM). The SEM micrographs in Figure 2 reveal that all samples, except P3, possess the characteristic macroporous and open-cell structure of polyHIPEs materials. Sample P3 has the characteristic void size but no interconnected pores (often termed windows) probably due to a too high stability of the HIPE with the Hypermer surfactant. The presence of large cells or macrocavities of several hundred μm in sample P4 **P5** is an indication that phase separation has occurred during the HIPE polymerization. The void size distributions derived from the SEM micrographs of the different samples are summarized in Table 3. The calculated porosity (Φ_{tot}) of the different polyHIPEs was estimated assuming complete removal of all the non-polymerizable components of the emulsion and compared to the experimental porosity (Φ_{exp}) obtained from mercury intrusion analysis (SI). Notably, samples P1, P4, and P5 exhibit a Φ_{exp} close to the corresponding theoretical value of 86 %, while a lower porosity was obtained for P2 probably due to the presence of closed pores (SEM see SI). While the distributions of pore size connections (windows) as determined by mercury porosimetry are relatively narrow for the majority of the samples and centered around 1.2-1.3 μm, sample P5 shows bimodal distribution and smaller pores size connections (836 nm and 289 nm) similar to what was ob-

served in SEM. The specific Brunauer, Emmet and Teller (BET) surface areas of the materials were recorded (SI). The values obtained were relatively high, between 168 and 758 m²/g due to the presence of mesopores in the materials. Sample P2 with a porogen in the HIPE formulation presents a very high content of mesopores with a diameter of pores two times greater (around 8 nm) than in the others samples. According to the literature, the replacement of some of the monomeric continuous phase with non-polymerisable solvent (porogen) such as toluene, produces a phase separation within the developing polymer structure between the internal phase droplets during polymerization.^{lvi,lvii} This leads to materials with dual porosity: very large macropores typical of polyHIPEs, with pore diameters above 1 μm, and much smaller pores within the polyHIPE walls.

In summary, polyHIPEs with good morphology could be obtained with both amine monomers...

Table 3 Structural characteristics of polyHIPEs supports.

sample	Φ_{tot} (a)	Φ_{exp} (b)	Void size (d) (μm)	Window diameter (b) (nm)	$S_{sp}^{(c)}$ (m ² /g)	Mesopore diameter (c) (nm)
P1	86	83	2-10	1256	413	4.65
P2	86	70	4-20	1338	171	7.86
P3	86	-	4-20	-	-	-
P4	86	81	2-20 + giants	1157	758	4.39
P5	86	81.5	1-5	660	168	4.46

(a) Total calculated porosity. (b) Estimated from mercury porosimetry. (c) Determined from nitrogen adsorption data using B.E.T. model. (d) Estimated from SEM micrograph.

The phthalimide protecting groups of sample P1 and P2 were removed by heating the polyHIPE with hydrazine monohydrate in ethanol resulting in amino functional polyHIPE (denoted as P1N and P2N). Attenuated total reflection FTIR spectra taken at different positions of cut monolithic samples revealed the disappearance of the characteristic C=O(N) band at 1718 cm⁻¹ consistent with the transformation of the phthalimide group to an amino group on the surface of the materials (Figure 3).

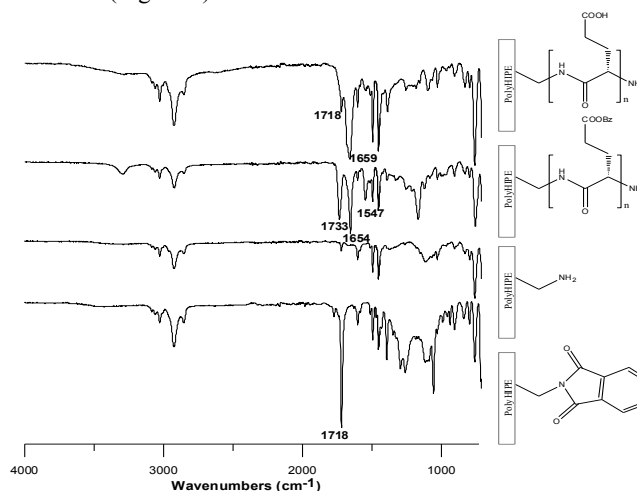


Figure 3. FTIR spectra of initial 4-vinylphthalimide based polyHIPE (P1), transformation into amino polyHIPE, after BLG NCA polymerization from polyHIPE with an initial weight ratio 200gm BLG / 40 gm amino polyHIPE, after final PBLG deprotection with TFA/HBr.

Grafting of polypeptides from amine functional polyHIPEs

The amine functional polyHIPEs were used for ring-opening polymerization of two amino acid NCAs from BLG and Lys(Z) to form polyHIPE grafted polypeptides. While elemental analysis confirmed the presence of amino groups in all polyHIPE samples (Table 4), the availability of a sufficient fraction of amino groups on the polyHIPE surface is critical for the success of the surface polymerization. The grafting reaction was systematically studied by immersing the polyHIPEs P1N, P2N (obtained with 4-vinylbenzylamine phthalimide), P4 and P5 (obtained with 4-vinylbenzylamine) in NCA solution of different concentrations. After intensive washing to remove all unbound polypeptide, the samples were analyzed to confirm the success of the surface polymerization. Figure 3 shows a typical FTIR spectrum of a cut monolithic sample after BLG polymerization. All spectra exhibit characteristic PBLG bands such as the carbonyl (1729 cm^{-1}), N-H (3295 cm^{-1}), α -helical amide I (1651 cm^{-1}) and amide II (1546 cm^{-1}) bands irrespective of the amino polyHIPE and the initial weight ratio of monomer to polyHIPE-NH₂ used. Several control experiments following the same washing procedure were carried out to provide evidence that the detected PBLG was indeed grafted. First, a polymerization of BLG NCA was initiated by a free initiator (benzylamine) in the presence of an inactive phthalimide protected polyHIPE but no PBLG was detected on the final polyHIPE. In a second control experiment 400 mg of free PBLG chains ($M_w = 37\,000\text{ g/mol}$, $D = 1.16$) were mixed in DMF with 40 mg polyHIPE-NH₂ (P1N) but again no PBLG could be detected after the washing procedure. These experiments signify the efficiency of the washing process and support the conclusion that the PBLG is indeed grafted on the polyHIPE surface rather than adsorbed or physical entrapped in the confined polyHIPE monolith.

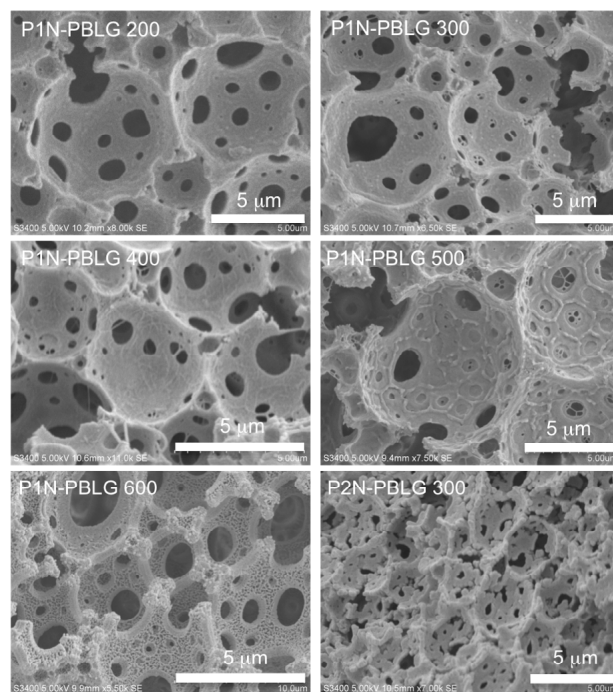


Figure 4. SEM images of polyHIPE-g-PBLG samples. The labels refer to the polyHIPE-NH₂ used and its ratio to BLG NCA (e.g. for P1N-PBLG 600 a weight ratio of P1N to BLG NCA of 600 was used).

Strong evidence for the success of the grafting reaction was also obtained from SEM analysis. While it was difficult to directly visualize the grafted PBLG layer on polyHIPEs synthesized from the 4-vinylbenzylamine samples P4 and P5 (SI), images obtained from polyHIPE-NH₂ derived from phthalimide formulations showed an apparent change in the surface morphology due to the presence of polymer (Figure 4). A clear change in surface roughness was observed when compared with the corresponding image of the polyHIPE-NH₂ suggesting a homogeneous PBLG layer on the polyHIPE surface. Moreover, the thickness of PBLG grafted on the surface by visual inspection appeared higher when the initial weight concentration of BLG NCA increased. The polyHIPE-g-PBLG was also analyzed by SEM in different zones, from the center to the external surface. The detailed visual examination confirmed that the polymerization occurs from all the surface of the monolith but it implies an increase in thickness of the PBLG layer from the center to the external surface (SI). This might be due to a lower monomer diffusion into the core of the polyHIPE-NH₂ during the polymerization. Interestingly, the images also revealed an unusual spider web-like pattern on the PBLG grafted surfaces specifically at higher initial ratios of BLG NCA to polyHIPE-NH₂ or near to the external surface (Figure 4). The exact reason for this is unknown, but it can be speculated that this is caused by the CO₂ gas evolution during polymerization. At high monomer concentration CO₂ might not be able to escape from the polyHIPE forming templating bubbles on the internal surface. This is supported by the observation that in some cases small fragments of polyHIPE were found in the reaction solution after one day of polymerization. This effect was more often observed with P2N polyHIPEs, which have a higher amount of surface amino group promoting faster monomer conversion and CO₂ evolution. It should be noted, though, that a homogeneous PBLG layer was formed in all samples and not just in patterns.

When Lys(Z) NCA was used as a monomer similar results were obtained (no patterns were observed). FTIR spectra confirmed the presence of PLys(Z) on all polyHIPEs irrespective of the polyHIPE-NH₂ used and the weight ratio of monomer to polyHIPE as evident from characteristic bands for N-H (3300 cm⁻¹), C=O (1696 cm⁻¹) and C-O band at 1244 cm⁻¹ attributed to the benzylcarbamate groups, and α -helical amide I (1650 cm⁻¹) and amide II bands (1538 cm⁻¹) (SI). From SEM analysis the PLys(Z) grafting appears more homogeneous than the PBLG grafting, probably due to a different rate of polymerization (Figure 5). Again, comparison of images taken at different spots suggests that a gradient in surface coverage also exists.

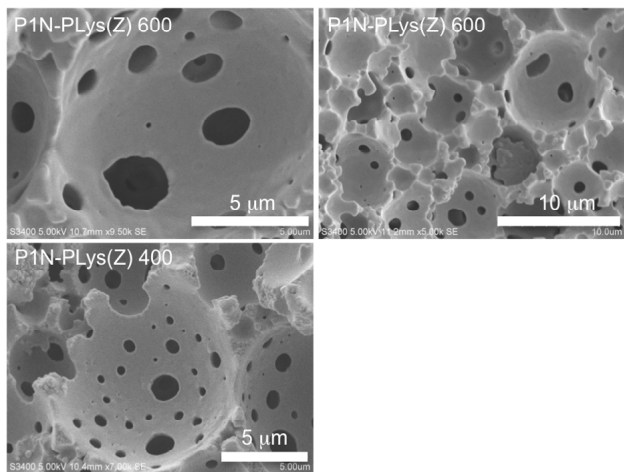


Figure 5. SEM pictures of different polyHIPE-g-PLys(Z) samples. The labels refer to the polyHIPE-NH₂ used and its ratio to BLG NCA (e.g. for P1N-PLys(Z) 400 a weight ratio of P1N to BLG NCA of 400 was used).

Table 4. Weight % of grafted polypeptide from elemental analysis.

sample	mg NCA per 40 mg pHIPE-NH ₂	% N normalized to C	wt% PGA ^(b)	wt% PLL ^(b)
P1N	-	1.47	-	-
P1N-PBLG ₂₀₀	200	7.24	30.5	-
P1N-PLys ₂₀₀	200	7.86	-	22.8
P1N-PBLG ₃₀₀	300	7.10	29.8	-
P1N-PLys ₃₀₀	300	8.24	-	24.2
P1N-PBLG ₄₀₀ ^(a)	400	10.01	45.16	-
P1N-PBLG ₄₀₀	400	3.83	12.5	-
P1N-PBLG ₅₀₀	500	5.87	23.3	-
P1N-PLys ₆₀₀	600	14.83	-	47.75
P1N-PBLG ₆₀₀ ^(a)	600	8.83	38.91	-
P1N-PBLG ₆₀₀	600	3.25	9.41	-
P2N	-	1.88	-	-
P2N-PBLG ₃₀₀	300	5.77	21.6	-
P2N-PLys ₄₀₀	400	10.46	-	30.6
P4	-	0.95	-	-
P4-PBLG ₂₀₀	200	2.03	5.7	-
P4-PLys ₂₀₀	200	2.83	-	6.7
P5	-	1.31	-	-

P5-PBLG ₂₀₀	200	3.46	11.4	-
P5-PLys ₂₀₀	200	2.98	-	6.0
P5-PBLG ₄₀₀	400	4.16	15.07	-
P5-PBLG ₄₀₀ ^(a)	400	4.59	17.35	-
P5-PLys ₄₀₀	400	3.95	-	9.4

(a) TMSI deprotection. (b) Calculated using the equation: wt% grafted polymer = 100 x (%N normalized to C in polyHIPE-g-polymer - (%N normalized to C in polyHIPE-NH₂)/%N normalized to C per unit polypeptide). The following calculated values were used: PGA: %N normalized to %C per unit polypeptide = 18.91; PLys the %N normalized to C per unit polypeptide = 28.

Elemental analysis was carried out on all polypeptide grafted samples to obtain quantitative information about the efficiency of the grafting and deprotection step. A good indicator is the amount of nitrogen in the sample introduced by the polypeptide grafting. For a better comparison the amount of nitrogen was normalized to the amount of carbon found in the polyHIPEs (Table 4). Generally, a greater amount of nitrogen (2-3 times higher) was found on the polyHIPE coated polypeptide from P1N and P2N resulting in a higher weight % of grafted PLL and PGA on the surface of the pHIPE. These results were in good agreement with the SEM images and suggest that using the protected 4-vinylphthalimide in the polyHIPE formulation results in more functional groups on the polyHIPE surface as compared to the unprotected 4-vinylphthalimide. Moreover, the amount of grafted PLL is increasing with the initial weight ratio of Lys(Z) NCA to pHIPE-NH₂. The presence of PLL on the surface of the monolith is perfectly visible by SEM (figure 8.a) analysis. Further evidence for the presence of the grafted polymer on the entire surface of the monolith was obtained from EDX oxygen mapping. The images clearly showed an increase of the amount of oxygen atoms originating from the polypeptides in the grafted monoliths (SI).

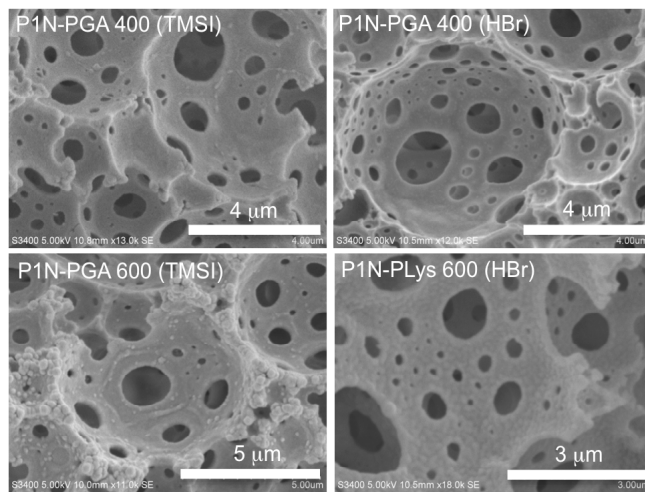


Figure 6. SEM pictures of deprotected polyHIPEs grafted polypeptides. The label denotes the polyHIPE-NH₂ used (e.g. P1N), the grafted polymer (e.g. Lys), the ratio of polyHIPE to NCA (e.g. 600) and the method of deprotection used (e.g. TMSI).

Functional polyHIPE surfaces were obtained by the subsequent deprotection of grafted PBLG and PLys(Z) polyHIPEs. The successful removal of the protecting groups of both grafted polymers can easily be monitored by FTIR spectroscopy though the disappearance of the benzylcarbamate bands at 1696 cm⁻¹ and 1248 cm⁻¹ for the PLys(Z) (SI) and the benzyl

ester band at 1733 cm^{-1} for the PBLG (SI), respectively. This process yielded $-\text{COOH}$ functional poly(glutamic acid) (polyHIPE-g-PGA) and $-\text{NH}_2$ functional poly(lysine) (polyHIPE-g-PLys) grafted polyHIPEs. After deprotection, the morphology of the polyHIPE was preserved and the cell and holes sizes appear more similar to those of the precursor monoliths due the significant mass loss ($\sim 40\%$) associated with the deprotection (Figure 6).

Interestingly, the amount of PGA found by elemental analysis appeared to be strongly dependant on the method of deprotection employed. For example, 9.41 weight % of PGA was found for the deprotection of P1N-PBLG₆₀₀ with HBr/TFA contrary to 38.91 % with trimethylsilyl iodide (TMSI)^{lxiii} process. This difference was also apparent both in SEM and FTIR analysis (SI). While the positions of the α -helical amide I and II remain unchanged after the deprotection with TMSI, in the case of HBr/TFA deprotection only the carboxylic acid band at 1713 cm^{-1} and an amide I band at 1677 cm^{-1} were visible. Apparently hydrolysis of the polypeptide occurs during HBr/TFA treatment as has been reported previously in the literature^{lix}, although it was noted that this did not happen with every sample. In summary, the best grafting results were obtained with... The presence of the grafted polypeptide does not have a large effect on morphology of the polyHIPEs, so that it is reasonable to assume similar flow characteristic.

Surface properties and conjugation

The grafting of a highly dense layer of functional polypeptides to the polyHIPE surface gives rise to changes in the macroscopic properties of the monoliths. Clear changes in the hydrophilicity could be induced in all polyHIPE grafted polypeptide (also those with low weight% grafting) by acidic/basic treatment (Figure 7). For example, a drop of water easily penetrated a polyHIPE-g-PLys at $\text{pH} < 7$ due to the protonation of the amino acid amine group, while treatment at $\text{pH} > 7$ rendered the material completely hydrophobic preventing the water from entering the monolith. The inversed pH-responsiveness was observed for the PGA grafted polyHIPEs. Amine functional polyHIPEs without any grafted polypeptides were not pH responsive and completely hydrophobic at any pH signifying the effect of the high density of functional surface groups introduced by the polypeptide grafting.

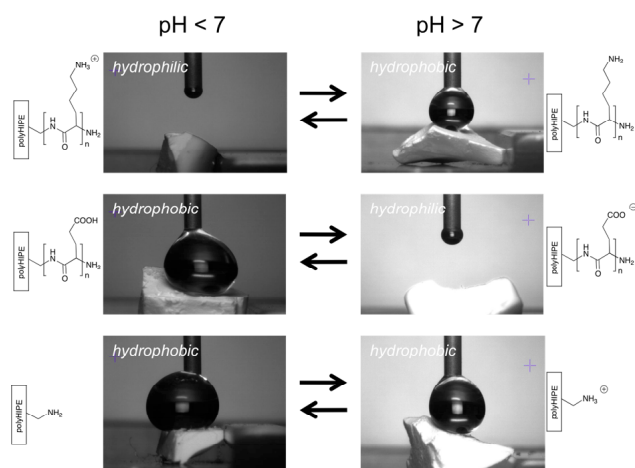


Figure 7. Change of hydrophilicity of polypeptide grafted polyHIPEs in response to pH visualized by placing a drop of water on the monolith. In case no drop is visible immediate penetration of the water into the polyHIPE occurred.

The open pore structure and high surface area of polyHIPEs makes them ideal materials for bioseparation applications. Bioconjugation was demonstrated in the past by covalent immobilization of proteins such as rAceGFP or CAL-B onto a functional polyHIPE.^{lx} PolyHIPE grafted PLL and PGA possess a much high density of amine and carboxylic acid functionalities, which may significantly enhanced their loading for bioconjugation. This was assessed in two model reactions. For polyHIPE-g-PLys conjugation was explored via surface coupling of fluorescein isothiocyanate (FITC). FITC is yellow-orange in color with an absorption maximum at 495 nm. Upon excitation it emits a yellow-green color with an emission maximum at 525 nm.^{lxi} Figure 8 shows that there was significantly more FITC conjugated to the polyHIPE-g-PLys than to the polyHIPE-NH₂ due to the greater amount of surface amines present in the former. FTIR data confirmed that no unreacted FITC was present in the final material by the absence of a band at 2100 cm^{-1} corresponding to the isothiocyanate group of FITC. FITC conjugation suggests that these amines localized on the pHIPE surface are reactive and can provide robust sites for further functionalization.

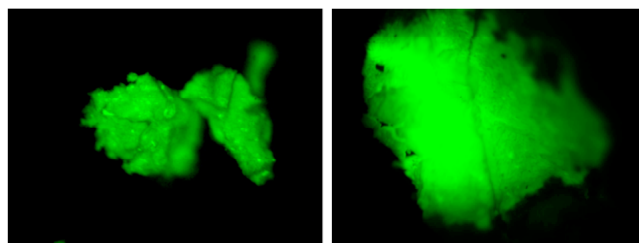


Figure 8. Microscopy images of FITC labeled polyHIPE-NH₂ PIN (left) and polyHIPE-g-PLys (deprotected PIN-PLys600, right).

Protein conjugation was investigated with the polyHIPE-g-PGA. Enhanced green fluorescent protein (eGFP) was selected for covalent immobilization as the immobilized protein can easily be visualized using commonly available filter sets designed for fluorescein and is among the brightest of the currently available fluorescent proteins.^{lxii} These features have rendered eGFP one of the most popular probes and the best choice for most single-label fluorescent protein experiments.^{lxiii, lxiv} The eGFP immobilization was realized by the reaction of a eGFP lysine residue with the carboxyl groups of grafted PGA in buffer solution using common EDC/sulfo-NHS coupling chemistry (Table 2). The success of the protein immobilization was visualized by blue-light exposure pictures. The images in Figure 9 clearly show that the eGFP modified materials are highly fluorescent throughout the samples. Noteworthy is that different apparent fluorescent intensities were observed: P3GFP and P4GFP are more fluorescent than P1GFP and P2GFP, which are more fluorescent than P5GFP.

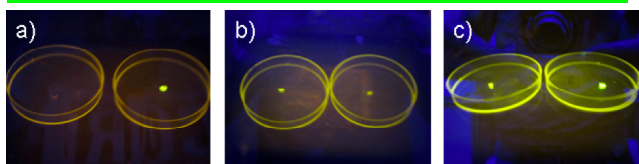


Figure 9. Pictures of functional polyHIPE-g-PGA immobilized eGFP exposed to a blue light source a) functional pHIPE before eGFP immobilization (control) and sample P3GFP b) samples P2GFP and P1GFP c) samples P4GFP and P3GFP3. Sample codes refer to Table 2 and denote polyHIPE-g-PGA used, e.g. P1GPF = P1-PGA.

Closer examination under a fluorescence optical microscope using a blue light filter also revealed green fluorescence in all PGA containing polyHIPEs conjugated with eGFP (Figure 10). No differences between the use of PBS or sodium carbonate buffer solution were observed. For the samples P3GFP and P4GFP a homogeneous fluorescence throughout the materials was only achieved at higher protein concentration compared to samples P1GFP and P2GFP. The sample P5GFP presents only fluorescence on the external surface of the pHIPE, due to a poor wettability of the material when the polyglutamic acid part is under the protonated form. WHAT ABOUT POLYHIPE-NH₂?

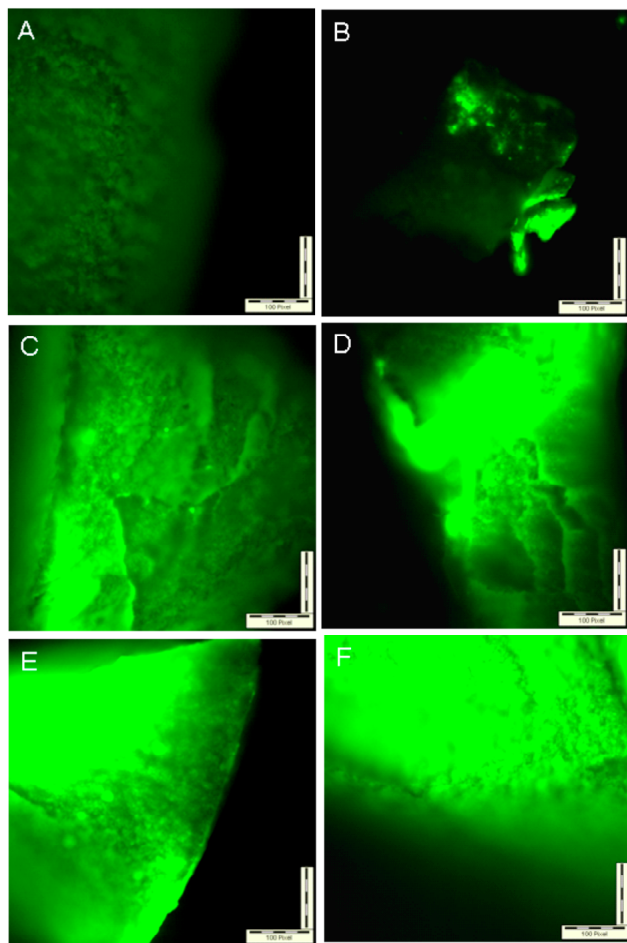


Figure 10. Fluorescence optical microscopy pictures at low exposure time (35 ms.) using a blue light filter. A) control (polyHIPE-g-PGA) B) sample P5GFP C) sample P2GFP D) sample P1GFP E) sample P3GFP F) sample P4GFP.

CONCLUSIONS

In this work a new class of functional macroporous polyHIPEs with tunable surface functional groups was disclosed. The obtained monoliths, based on styrenic monomers, thermal initiator and an amine functional monomer present the expected open-cell morphology and a high surface area. The incorporated amino group was successfully used to initiate the ring opening polymerization of benzyl-L-glutamate (BLG) NCA and benzyloxycarbonyl-L-lysine (Lys(Z)) NCA, which resulted in a dense coating of polypeptides on the polyHIPE surface. The amount of polypeptide grafted to the polyHIPE surfaces could be modulated by varying the initial ratio of amino acid NCA to polyHIPE-NH₂. Subsequent removal of the polypeptide

protecting groups yielded highly functional polyHIPE-g-poly(glutamic acid) and polyHIPE-g-poly(lysine). Both types of polypeptide-grafted monoliths responded to pH by changes in their hydrophilicity. The possibility to use the high density of function (-COOH or -NH₂) for secondary reaction was demonstrated by the successful conjugation of enhanced green fluorescent protein and FITC on the polymer 3D-scaffold surface. The materials and methodologies presented here open new potential in biosensor as well as in bioseparation applications for highly functional polyHIPEs.

ASSOCIATED CONTENT

Supporting Information. A brief statement in nonsentence format listing the contents of material supplied as Supporting Information should be included, ending with "This material is available free of charge via the Internet at <http://pubs.acs.org>." For instructions on what should be included in the Supporting Information as well as how to prepare this material for publication, check the Instructions for Authors at <http://pubs.acs.org/page/jacsat/submission/authors.html>.

AUTHOR INFORMATION

Corresponding Author

* email: andreas.heise@dcu.ie. Tel: 00353-1-7006709. Fax: 00353-1-7005503.

ACKNOWLEDGMENT

F.A. would like to thank the European Commission for funding this work under Marie-Curie Intra-European Fellowship program "Highly Functional Porous Materials for Bio-Diagnostic Sensors" (PoroSens, contract No. PIEF-GA-2009-252862). Financial support from the Science Foundation Ireland (SFI) Principle Investigator Award 07/IN1/B1792 (J.H. and A.H.) is gratefully acknowledged. AH is a SFI Stokes Senior Lecturer (07/SK/B1241). ISSC The authors thank Dr. Brendan Twamley for his help in EDX measurements. The authors also thank Odile Babot from the Institut des Sciences moléculaires, University of Bordeaux I, for BET and Hg intrusion porosimetry analysis.

REFERENCES

- ⁱ Kimmins, S. D.; Cameron, N. R. *Adv. Funct. Mater.* **2011**, *21*, 211.
- ⁱⁱ Krajnc, P.; Leber, N.; Stefanec, D.; Kontrec, S.; Podgornik, A. *J. Chromatogr., A* **2005**, *1065*, 69.
- ⁱⁱⁱ Tunc, Y.; Gogelioglu, C.; Hasirci, N.; Ulubayram, K.; Tuncel, A. *J. Chromatogr., A* **2010**, *1217*, 1654.
- ^{iv} Pulko, I.; Smrekar, V.; Podgornik, A.; Krajnc, P. *J. Chromatogr., A* **2011**, *1218*, 2396.
- ^v Barbetta, A.; Massimi, M.; Devirgiliis, L. C.; Dentini, M. *Biomacromolecules* **2006**, *7*, 3059.
- ^{vi} Busby, W.; Cameron, N. R.; Jahoda, C. A. B. *Biomacromolecules* **2001**, *2*, 154.
- ^{vii} Su, F.; Bray, C. L.; Tan, B.; Cooper, A. I. *Adv. Mater.* **2008**, *20*, 2663.
- ^{viii} Moglia, R. S.; Holm, J. L.; Sears, N. A.; Wilson, C. J.; Harrison, D. M.; Cosgriff-Hernandez, E. *Biomacromolecules* **2011**, *12*, 3621.
- ^{ix} Barby, D.; Haq, Z. *European Patent 60 138*, March, 3, **1982**.
- ^x Cameron, N. R.; Sherrington, D. C. *Adv. Polym. Sci.* **1996**, *126*, 163.
- ^{xi} Cameron, N. R.; Sherrington, D. C. *Macromolecules* **1997**, *30*, 5860.
- ^{xii} Ko, Y. C.; Lindsay, J. D. *World Patent 044 041*, May 27, **2004**.

- ^{xiii} Barbetta, A.; Dentini, M.; Zannoni, E. M.; De Stefano, M. *Langmuir* **2005**, *21*, 12333.
- ^{xiv} Barbetta, A.; Dentini, M.; De Vecchi, M. S.; Filippini, P.; Formisano, G.; Gaiazzo, S. *Adv. Funct. Mater.* **2005**, *15*, 118.
- ^{xv} Krajnc, P.; Stefanec, D.; Pulko, I. *Macromol. Rapid Commun.* **2005**, *26*, 1289.
- ^{xvi} Besnard, O.; Pasquinet, E.; Birot, M.; Deleuze, H.; Audouin, F. *World Patent 15 0113 (A1)*, Dec. 19, **2009**.
- ^{xvii} Youssef, C.; Backov, R.; Treguer, M.; Birot, M.; Deleuze, H. *J. Polym. Sci., Part A: Polym. Chem.* **2010**, *48*, 2942.
- ^{xviii} Audouin, F.; Birot, M.; Pasquinet, E.; Besnard, O.; Palmas, P.; Poullain, D.; Deleuze, H. *Macromolecules* **2011**, *44*, 4879.
- ^{xix} Gokmen, M. T.; Van Camp, W.; Colver, P. J.; Bon, S. A. F.; Du Prez, F. E. *Macromolecules* **2009**, *42*, 9289.
- ^{xx} Leber, N.; Fay, J. D. B.; Cameron, N. R.; Krajnc, P. *J. Polym. Sci., Part A: Polym. Chem.* **2007**, *45*, 4043.
- ^{xxi} Lucchesi, C.; Pascual, S.; Dujardin, G.; Fontaine, L. *React. Funct. Polym.* **2008**, *68*, 97.
- ^{xxii} Kovacic, S.; Krajnc, P.; Slugovc, C. *Chem. Commun.* **2010**, *46*, 7504.
- ^{xxiii} Deleuze, H.; Maillard, B.; Mondain-Monval, O. *Bioorg. Med. Chem. Lett.* **2002**, *12*, 1877.
- ^{xxiv} Fernandez-Trillo, F.; Van Hest, J. C. M.; Thies, J. C.; Michon, T.; Weberskirch, R.; Cameron, N. R. *Adv. Mater.* **2009**, *21*, 55.
- ^{xxv} Barbey, R.; Lavanant, L.; Paripovic, D.; Schüwer, N.; Sugnaux, C.; Tugulu, S.; Klok, H.-A. *Chem. Rev.* **2009**, *109*, 5437.
- ^{xxvi} Moine, L.; Deleuze, H.; Degueil, M.; Maillard, B. *J. Polym. Sci., Part A: Polym. Chem.* **2004**, *42*, 1216.
- ^{xxvii} Cummins, D.; Wyman, P.; Duxbury, C. J.; Thies, J.; Koning, C. E.; Heise, A. *Chem. Mater.* **2007**, *19*, 5285.
- ^{xxviii} Cummins, D.; Duxbury, C. J.; Quaedflieg, P. J. L. M.; Magusin, P. C. M. M.; Koning, C. E.; Heise, A. *Soft Matter* **2009**, *5*, 804.
- ^{xxix} Carlsen, A.; Lecommandoux, S. *Curr. Opin. Colloid Interface Sci.* **2009**, *14*, 329.
- ^{xxx} Borase, T.; Iacono, M.; Ali, S. I.; Thornton, P. D.; Heise, A. *Polym. Chem.* **2012**, *3*, 1267.
- ^{xxxi} Habraken, G. J. M.; Koning, C. E.; Heuts, J. P. A.; Heise, A. *Chem. Commun.* **2009**, *24*, 3612.
- ^{xxxii} Huang, J.; Habraken, G.; Audouin, F.; Heise, A. *Macromolecules* **2010**, *43*, 6050.
- ^{xxxiii} Engler, A. C.; Hyung-il Lee, Hammond, P. T. *Angew. Chem. Int. Ed.* **2009**, *48*, 9334.
- ^{xxxiv} Sun, J.; Schlaad, H. *Macromolecules* **2010**, *43*, 4445.
- ^{xxxv} Tang, H.; Zhang, D. *Biomacromolecules* **2010**, *11*, 1585.
- ^{xxxvi} Hadjichristidis, N.; Iatrou, H.; Pitsikalis, M.; Sakellariou, G. *Chem. Rev.* **2009**, *109*, 5528.
- ^{xxxvii} Habraken, G. J. M.; Heise, A.; Thornton, P. D. *Macromol. Rapid Commun.* **2012**, *33*, 272.
- ^{xxxviii} Gibson, M. I.; Cameron, N. R. *Angew. Chem., Int. Ed.* **2008**, *47*, 5160.
- ^{xxxix} Klok, H.-A.; Lecommandoux, S. *Adv. Polym. Sci.* **2006**, *202*, 75.
- ^{xl} Schlaad, H. *Adv. Polym. Sci.* **2006**, *202*, 53.
- ^{xli} Deming, T. J. *Nature* **1997**, *390*, 386.
- ^{xlii} Dimitrov, I.; Schlaad, H. *Chem. Commun.* **2003**, 2944.
- ^{xliiii} Lu, H.; Cheng, J. J. *J. Am. Chem. Soc.* **2007**, *129*, 14114.
- ^{xliiii} Kricheldorf, H. R. *Angew. Chem. Int. Ed.* **2006**, *45*, 572.
- ^{xlv} Habraken, G. J. M.; Koning, C. E.; Heise, A. *J. Polym. Sci., Part A: Polym. Chem.* **2009**, *47*, 6883.
- ^{xlvii} Audouin, F.; Knoop, R. J. I.; Huang, J.; Heise, A. *J. Polym. Sci., Part A: Polym. Chem.* **2010**, *48*, 4602.
- ^{xlviii} Brunauer, S.; Emmett, P. H.; Teller, E. *J. Am. Chem. Soc.* **1938**, *60*, 309.
- ^{xlviii} Carnachan, R. J.; Bokhari, M.; Przyborski, S.; Cameron, N. R. *Soft Matter* **2006**, *2*, 608.
- ^{xlix} Livshin, S.; Silverstein, M. S. *Macromolecules* **2008**, *41*, 3930.
- ^l Schwab, M. G.; Senkovska, I.; Rose, M.; Koch, M.; Pahnke, J.; Jonschker, G.; Kaskel, S. *Adv. Eng. Mater.* **2008**, *10*, 1151.
- ^{li} Leber, N.; Fay, J. D. B.; Cameron, N. R.; Krajnc, P. *J. Polym. Sci., Part A: Polym. Chem.* **2007**, *45*, 4043.
- ^{lii} Jerabek, K.; Pulko, I.; Soukupova, K.; Stefanec, D.; Krajnc, P. *Macromolecules* **2008**, *41*, 3543.
- ^{liii} Barbetta, A.; Cameron, N. R. *Macromolecules* **2004**, *37*, 3202.
- ^{liiii} Barbetta, A.; Dentini, M.; Leandri, L.; Ferraris, G.; Coletta, A.; Bernabei, M. *React. Funct. Polym.* **2009**, *69*, 724.
- ^{lv} Lovelady, E.; Kimmins, S. D.; Wu, J.; Cameron, N. R. *Polym. Chem.* **2011**, *2*, 559.
- ^{lvi} Hainey, P.; Huxham, I. M.; Rowatt, B.; Sherrington, D. C. *Macromolecules* **1991**, *24*, 117.
- ^{lvii} Barbetta, A.; Cameron, N. R. *Macromolecules* **2004**, *37*, 3188.
- ^{lviii} Subramanian, G.; Hjelm, R. P.; Deming, T. J.; Smith, G. S.; Li, Y.; Safinya, C. R. *J. Am. Chem. Soc.* **2000**, *122*, 26.
- ^{lix} Blout, E. R.; Idelson, M. *J. Am. Chem. Soc.* **1956**, *78*, 497.
- ^{lx} Pierre, S. J.; Thies, J. C.; Dureault, A.; Cameron, N. R.; van Hest, J. C. M.; Carrette, N.; Michon, T.; Weberskirch, R. *Adv. Mater.* **2006**, *18*, 1822.
- ^{lxi} Orndorff, W. R.; Hemmer, A. J. *J. Am. Chem. Soc.* **1927**, *49*, 1272.
- ^{lxii} Heim, R.; Cubitt, A.; Tsien, R. *Nature* **1995**, *373*, 663.
- ^{lxiii} Cormack, B. P.; Valdivia, R.; Falkow, S. *Gene* **1996**, *173*, 33.
- ^{lxiv} Tsien, R. *Ann. Rev. Biochem.* **1998**, *67*, 509.

Insert Table of Contents artwork here